ATLAS Internal Note
MUON-NO-033
13 January 1994

Preprint PNPI
1941 Dec. 1993

Differential sensitivity of cathode strip chambers to neutrons and photons

A.S.Denisov, A.A.Fetisov, L.P.Lapina, A.B.Laptev, V.P.Maleev
M.A.Nesvizhevskaja, O.A.Shcherbakov, A.G.Sergeev, A.I.Smirnov,
V.M.Suvorov, A.A.Vorobyov, A.V.Zhelamkov

Petersburg Nuclear Physics Institute
December 18, 1993

Abstract

We investigated the response of the CSC to neutrons in the energy range 0.4 eV $< E_n <$ 100 KeV using the Gatchina time of flight neutron spectrometer GNEIS. Also, we have measured the sensitivity of the CSC's to gammas of the different energies using a set of the gamma radioactive sources.

1. Introduction

The muon chambers for the GEM detector should operate in environment of substantial background of neutrons and associated photons. Therefore it is important to know the sensitivity of the muon chambers to neutrons and photons because the rate of the interactions induced by these particles may affect the muon trigger rate and the pattern recognition efficiency and hence will determine the detector concept and the efforts on shielding [1].

The spectrum of neutrons at GEM muon detector spans from 0.1 eV to 1 MeV for the shielded detector [1]. Therefore in order to estimate the muon chamber rates caused by the neutron background one should know the sensitivity of CSC's to neutrons in a wide energy range mentioned above.

The neutron associated photons produced mainly by the (n,γ) reactions have the energies in the range of 0.1< E_γ <10 MeV. Their spectrum is peaking at the energy about 0.1 MeV.

We have measured the differential sensitivity to neutrons the CSC's designed for GEM using the Gatchina TOF neutron spectrometer GNEIS [2]. Also, we measured sensitivity of the CSC to gammas of various radioactive sources.

2. Experimental setup.

The schematic layout of neutron measurements and the GNEIS facility are shown in fig. 1. The TOF spectrometer is based on the 1 GeV PNPI proton synchrotron [3]. Fast neutrons are produced when the proton beam inflicts on the lead target placed below the median plane of the accelerator magnetic field. Low energy neutrons are emitted from the polyethylene moderator located above the median plane. The whole target/moderator assembly is inside the accelerator vacuum chamber. There are five holes for neutrons through the 6 m thick accelerator shielding wall. The five flight paths are arranged so that the four of them look at the moderator and the fifth one looks at the lead target producing fast neutrons. The collimator system of the spectrometer consist of the brass and iron collimators (K_1, K_2) and of brass, lead and borated polyethylene jaws located inside the neutron guide tubes. Measurement station are situated at flight path distances of 35–50 m in the experimental building.

The main parameters of the GNEIS facility are as follows:

proton beam energy	1 Gev
average proton beam current	2.3 μA
pulse width	10 nsec
total neutron flux	$3 \cdot 10^{14}$ n/sec
repetition rate	< 50 Hz

We used the $N3$ neutron beam for the neutron tests. The neutron energies for this direction span from 0.4 eV to 100 KeV. Neutrons below 0.4 eV were captured by the 1 mm thick Cd foil at the entrance of the TOF path.The start pulse was produced by the gamma ray burst from the lead target detected by a scintillation counter.

The TOF spectra of neutrons and the neutron beam intensity were measured by the standard ionization chamber filled with the ^{3}He(3 atm)+Ar(3 atm)+ CO_2(3 torr) gas mixture. The chamber detection efficiency to neutrons was calculated on the base of the chamber sensitive length (60 mm), the ^{3}He(n,p)^{3}H reaction cross section known with high accuracy [4] and the measured efficiency of the chamber electronics.

The TOF electronics and the data acquisition system of the ^{3}He chamber were described in [2]. The energy calibration of the spectrometer was done by putting the materials with well known neutron resonances (Mn,Ag,In) in the neutron beam upstream of the ^{3}He chamber. We used a usual proportional gas counter with BF_3 as a monitor.

The neutron test setup is shown in the upper right corner of fig. 1. In addition to the CSC module and the ^{3}He chamber we used a thin walled proportional chamber (TWPC) and two scintillation counters to suppress the charge particle contamination of beam and a BGO gamma detector to control the beam gamma component.

The CSC module consisted of four chambers shown in fig 2. The sensitive area of CSC's was 75×75 mm^2. All the cathode strips from every CSC's were joined together and connected with the input of charge sensitive amplifier. Similarly, the anode wires from each CSC were joined together.

The chambers were filled with the $50\%CO_2+30\%Ar+20\%CF_4$ gas mixture at atmospheric pressure and operated in proportional mode at HV = 2.5 KV. The threshold of the hit registration was set to 0.8 KeV of the electron energy loss in the sensitive volume. The threshold was determined from the position of 5.9 KeV ^{55}Fe peak in the special thin walled proportional chamber at the same geometry. The charge sensitive preamplifiers for the anodes and cathodes had the integration time about 50 nsec. The preamplifier dead time was 70 nsec. The sensitivity threshold of each preamplifier was 20 fC approximately.

It was required that the signals from the cathode should coincide with the anode signals in each chamber independently. There were 4 readout channels of proportional chambers (CH1÷CH4). The arrival time of the signal and its amplitude were measured in each channel. Also, counting rates from scintillation counters (S1–S2) as well as from BGO detector and from BF_3 monitor were measured.

3. Procedure of the neutron measurement. Results.

The problem of the neutron test is that the neutron beam is contaminated by gammas which are detected by CSC's with the efficiency ten times higher than neutron efficiency. To select the neutron contribution we measured the TOF spectra of CSC's and ^{3}He chamber with and without the 25 mm thick polyethylene filter in the beam at 6 m upstream the chamber. The filter inserted at this distance works as a neutron scatterer. The TOF spectra over four CSC are presented in fig. 3 a,b,c,d. The average value of the counting rate without filter is a factor of 1.15 higher than the rate with the filter. One can see remarkable resonance structure (fig. 3 b,c) induced by the (n,γ) reactions on the Br isotopes contained in the G10 material.

Fig. 4 presents the TOF spectra in the ^{3}He chamber with and without filter. The overall ^{3}He counting rate reduced by the filter more than 35 times. This suppressing varies in different neutron spectrum regions. It is about 10 for 10–100 KeV and more than 100 for the low energy end.

The difference between TOF spectra of CSC's was measured with the open and filtered beams. It contains also the contribution from gammas. It means that the filtered TOF spectra before subtraction from the unfiltered one should be increased to take into account the contribution from gammas scattered by filter. The correction factor was calculated from the BGO integral counting rate over the whole time interval measured in every run and from BGO signal time spectra measured with and without filter. The sensitivity of the BGO spectrometer to neutron is essentially less than to gammas. We have measured also the TOF spectra of CSC's with a 50 mm thick polyethylene filter in the beam. The difference between the CSC responses for the beams filtered by 25 mm and 50 mm was used for correction factor due to gamma scattering in the 25 mm filter. The two methods gave us the same values of the correction factor: 1.1.

The neutron flux interacting with the CSC's was obtained from the difference between two ^{3}He TOF spectra measured with and without 25 mm polyethylene in the beam and calculated efficiency of ^{3}He chamber.

With the neutron flux and corrected difference between the two TOF spectra of the CSC's we can determine differential detection efficiency of the CSC to neutrons presented in table 1 and shown in fig. 5.

The sensitivity of the GEM CSC prototype to neutrons was measured independently by ITEP group [6] for the thermal neutrons (efficiency $6.5 \cdot 10^{-4}$) and fast neutrons with the energy averaged over range 0.1 MeV $< E_n <$ 10 MeV (efficiency $2 \cdot 10^{-4}$) using ^{252}Cf source.

Our efficiency value for 0.4–1 eV neutrons is not in disagreement with the ITEP results if one take into account the 1/v dependence of the cross section for low energy neutrons.

On the high energy end we observe the rise of the efficiency from $0.07 \cdot 10^{-4}$ for 10^3–10^4 eV energy interval to $0.5 \cdot 10^{-4}$ for 10^4–10^5 eV energy neutrons. This rise can be an indication that the neutron elastic scattering on the gas nuclei begin to contribute detection efficiency in the 10^4–10^5 eV energy interval. According to [6,7] the efficiency due to scattering on gas nuclei reaches the maximum value at the neutron energy of about 1 MeV, the main mechanism of neutron detection being the elastic scattering of neutrons on gas nuclei, so our rise of detection efficiency and its value for 10^4–10^5 eV is not contradict the ITEP data.

The observed increase of the efficiency for 10–10^2 eV neutron energy range is related with the contribution of the Br isotopes (n,γ) resonances.

We have measured also the correlated efficiencies for the double and triple coincidences between CSC's of the stack.

The efficiency of the coincidences between two neighbor chambers is $(1.9 \pm 0.7) \cdot 10^{-6}$. This value is 10^2 times less than efficiency of the single chamber but is 10^2 times higher than the pure accidental rate. In any case this value is acceptable for the practical utilization of the CSC's in GEM.

The efficiency of coincidences between CSC1 and CSC3 was $(8 \pm 3) \cdot 10^{-7}$.

The efficiency for the triple coincidence of the neighbor chambers was less than 10^{-7}.

The main result of these measurements can be formulated as follows:

1. The sensibility of CSC's to neutrons in the energy range 0.4 eV—100 KeV is an order of magnitude less than it was assumed before in the GEM Muon System project.

2. The correlated efficiencies of various combination of the CSC's proved to be quite low.

These conclusions mean that neutron background in GEM could not spoil the performance of the CSC's in the Muon System.

4. CSC efficiency to gammas.

Detection efficiency of CSCs to gamma radiation of different energies was measured using calibrated radioactive sources with activities known to 1,5÷2,0 % accuracy. The geometry of the experiment is shown in fig. 2.

The aluminum filters were used for absorption of the electrons from the sources. We took into account that the CSC front walls (2 plates of G10 covered by copper) are not transparent for photons with energy lower than $\sim$ 20 KeV and electrons with energy below $\sim$ 1 MeV. The list of the sources and the filter thicknesses are presented in table 2 together with the measured efficiencies ε_γ. The values of ε_γ are plotted in fig. 6 as function of photon energy.

Several remarks about the measurements and the results:

1. The sources ^{54}Mn,^{57}Co,^{60}Co,^{241}Am have practically monoenergetic γ–spectra, the soft x-rays being completely absorbed by the front walls of the CSC. So the counting rates

give us directly the absolute values of the CSC efficiencies for corresponding energies. The sources ^{109}Cd,^{113}Cs,^{139}Ce have also the monoenergetic γ–lines, but the energy of the x-rays associated with the radioactive decays is quite big: 22,5 ÷ 34 KeV. In these cases the efficiencies ε_γ and ε_x can be evaluated from the measurements with and without filters. In such a way 12 values of $\varepsilon_\gamma(E_\gamma)$ were obtained in the region E = 22.5÷1250 KeV. In addition, the sources ^{88}Y and ^{228}Th with more complicated gamma-spectra have been used. ^{88}Y has two strong γ–lines: 898 KeV and 1835 KeV. The contribution of 898 KeV gammas to the counting rate was evaluated from the known value of ε_γ(898 KeV), and so we found ε_γ(1835 KeV). The ^{228}Th source has a strong γ–line of 2614 KeV and complicated γ–spectra in the region of $E_\gamma \leq$1620 KeV. However the contribution of the "soft" part of the spectrum was only 1/4 of the total counting rate. The ^{134}Ba source was used for determination of ε_γ(31.4 KeV).

2. The efficiency of CSC to gammas is associated mainly with secondary electrons emitted from construction materials into the gas gap. The contribution of the gas gap itself to the efficiency is small as shown in fig. 6.

3. The observed dependence of the CSC efficiency on the photon energy is the result of competition between two effects: decreasing of the photon absorption cross section with energy and increasing of the penetrability of the secondary electrons. In the region of 30÷200 KeV the photoeffect from the copper cathodes plays decisive role in the chamber efficiency. The cross section of the photoeffect is proportional to $\sim E_\gamma^{-3}$ while the range of the electrons depends on the energy as $\sim E_e^{1.6}$. This fact explains the negative slope of dependence for E_γ <300 KeV. Roughly speaking it should be as $\sim E_\gamma^{-1.4}$. For E_γ >300 KeV the compton effect in the wall material dominates. The cross section of this process decreases slowly ($\sim E_\gamma^{-0.25}$). This is the reason for the efficiency rise in the high energy region.

   The energy dependence of the efficiency is in qualitative accordance with data for secondary electron yields from solids irradiated by gammas [8]. In fig. 7 the experimental data taken from [8] are presented for the case of secondary electron yield $\eta(E_\gamma)$ from copper. Also the results of several Monte-Carlo calculations are shown.

4. It should be mentioned that the aluminum filters can distort the measurements due to fast secondary elections from the filter itself. This effect was estimated for E_γ= 2614 KeV using the data from ref [8] on the forward electron yield for aluminum (η(2614 KeV) = 10^{-2} electrons/photon) and on the spatial-energy distribution of these electrons. The result is that only $4\cdot10^{-4}$ electrons per photon from the aluminum filter can reach the gas gap of the CSC. The corrected value for efficiency is ε_γ(2614 KeV) = $(17\pm3)\cdot10^{-3}$ counts/photon. The correction for E_γ <1900 KeV was small and it was not taken into account. In case of^{88}Y this was checked experimentally: the counting rate from ^{88}Y source was the same for the measurements with the 0,5cm aluminum filter and without.

These measurements demonstrate that the efficiency of the CSC's to gammas is much higher than to neutrons, and it should be seriously taken into account while considering the performance of the GEM muon system.

Bibliography

1. GEM TN–93–262, Technical Design Report, April 1993
2. O.L.Fedin et al., GEM TN–93–352, March 1993
3. N.K.Abrosimov et al., Nucl.Instrum.and Meth., A242 (1985) 121
4. N.K.Abrosimov et al., J.Techn.Phys., 41 (1971) 1969
5. Drake M.K. "ENDF/B–111 Cross Section Measurements Standards", BNL 17188 (ENDF–179), 1972
6. S.Boyarinov et al., GEM TN-93-345,June 1993
7. GEM TN–93–299, February 1993
8. A.F.Akkerman, M.Ya.Grudskii,V.V.Smirnov. Secondary electron emission from solids irradiated by gammas. Moscow,Energoatomisdat,1986

Table 1. Efficiency of CSC to neutrons.

Energy interval (eV)	Efficiency ε_n ($\times 10^{-4}$)
0.4—1	1.27 ±0.35
1—10	0.90 ± 0.09
10—10^2	1.14 ± 0.09
10^2—10^3	0.68 ± 0.08
10^3—10^4	0.07 ± 0.05
10^4—10^5	0.50 ± 0.04

Table 2. Radioactive sources, filters and gamma efficiencies.

Source	Eγ(KeV)	Al filter (cm)	Efficiency ε_γ ($\times 10^{-3}$)
^{54}Mn	834.8	0 and 0.1	3.5 ± 0.2
^{57}Co	135 *	0 and 0.5	1.8 ± 0.2
^{60}Co	1250 *	0 and 0.5	6.36 ± 0.12
^{88}Y	1836	0 and 0.5	10 ± 1
^{109}Cd	K_α 22.5	0	1.05 ± 0.05
	88.0	1.0	2.6 ± 0.3
^{113}Sn	K_α 24.7	0	1.7 ± 0.4
	391.7	1.0	1.4 ± 0.4
^{133}Ba	K_α 31.6	0 and 1.0	4.2 ± 0.4
^{137}Cs	K_α 32.9	0	6.1 ± 1.6
	661.6	1.9	2.6 ± 0.2
^{139}Ce	K_α 34.1	0	3.7 ± 0.4
	165.8	1.9	1.1 ± 0.3
^{228}Th	2614	0.5	[21 ± 2]
			17 ± 3 **
^{241}Am	59.5	0.5	3.25 ± 0.12

* Average values for doublets of close γ–lines.

** The value is corrected for secondary electrons from Al filters.

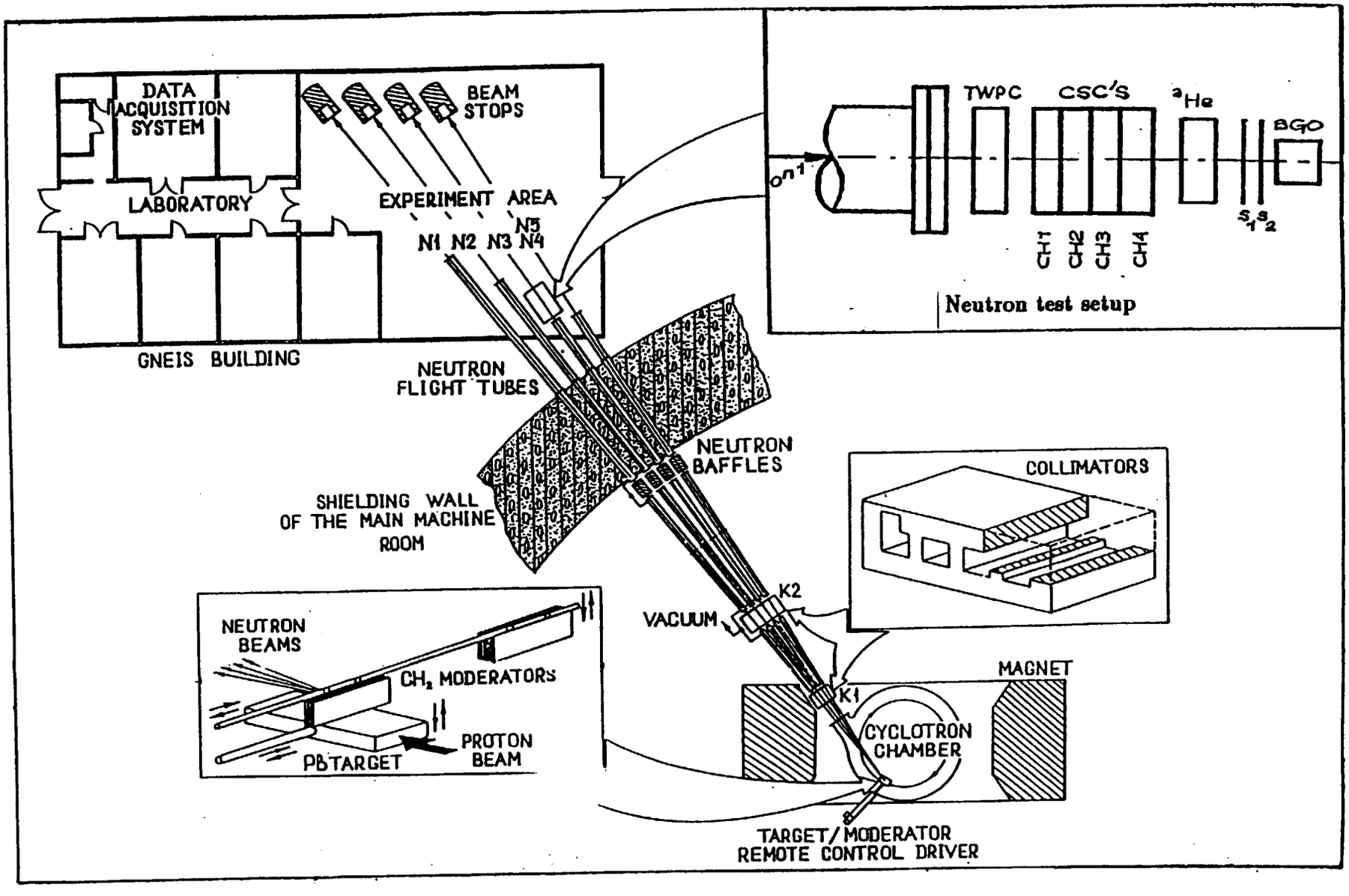

Fig.1 General layout of the GNEIS facility

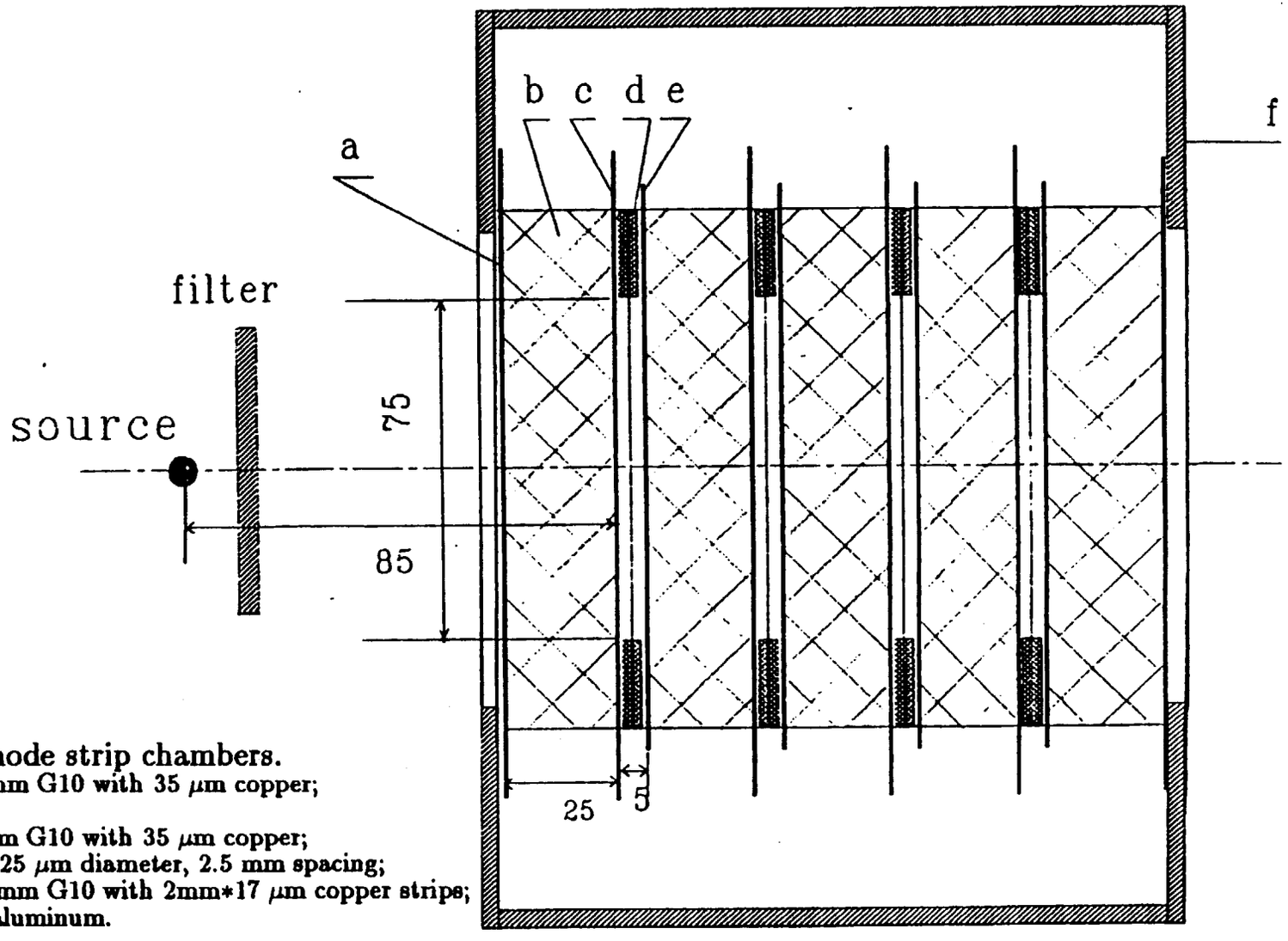

Fig.2 Cathode strip chambers.

a - Window,0.5 mm G10 with 35 μm copper;
b - Hexcel;
c - Cathode, 1 mm G10 with 35 μm copper;
d - Anode wires, 25 μm diameter, 2.5 mm spacing;
e - Cathode, 1.2 mm G10 with 2mm*17 μm copper strips;
f - Filter, 5 mm aluminum.

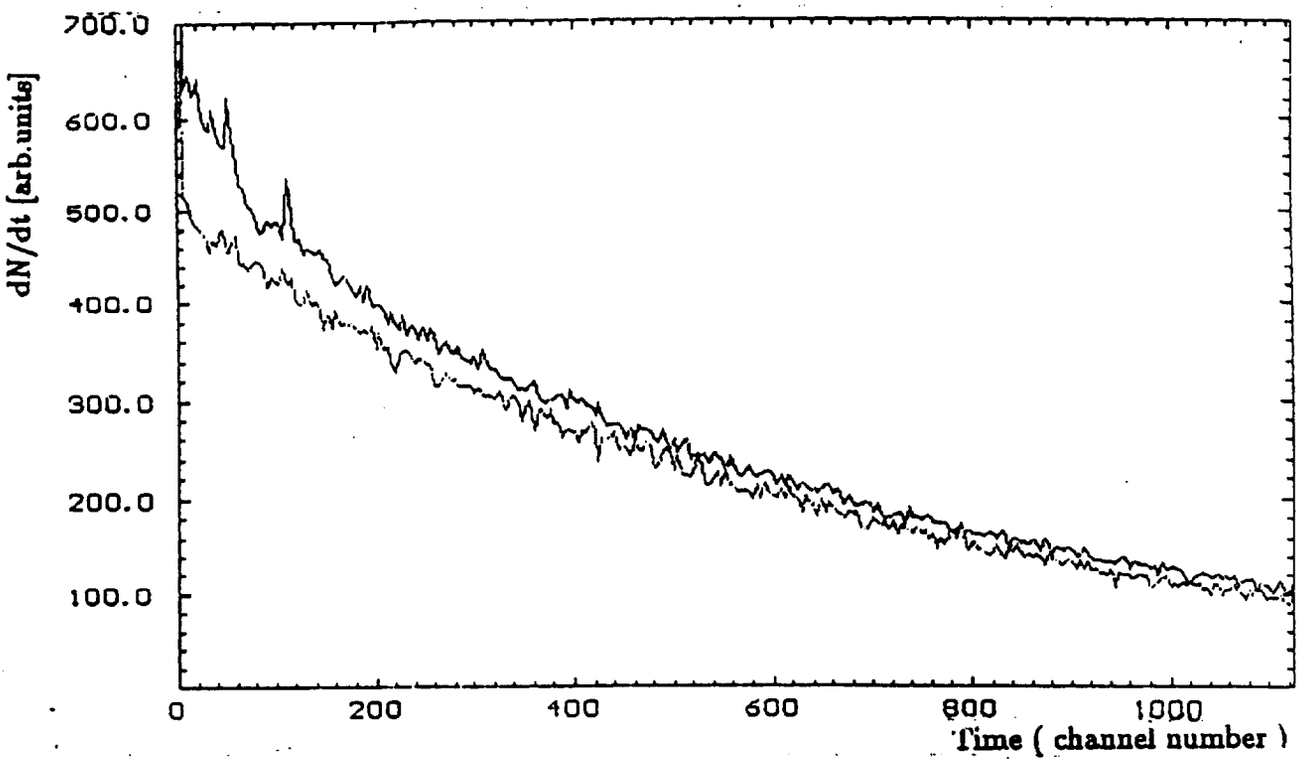

Fig.3 a. CSC TOF spectra with and without filter in the beam

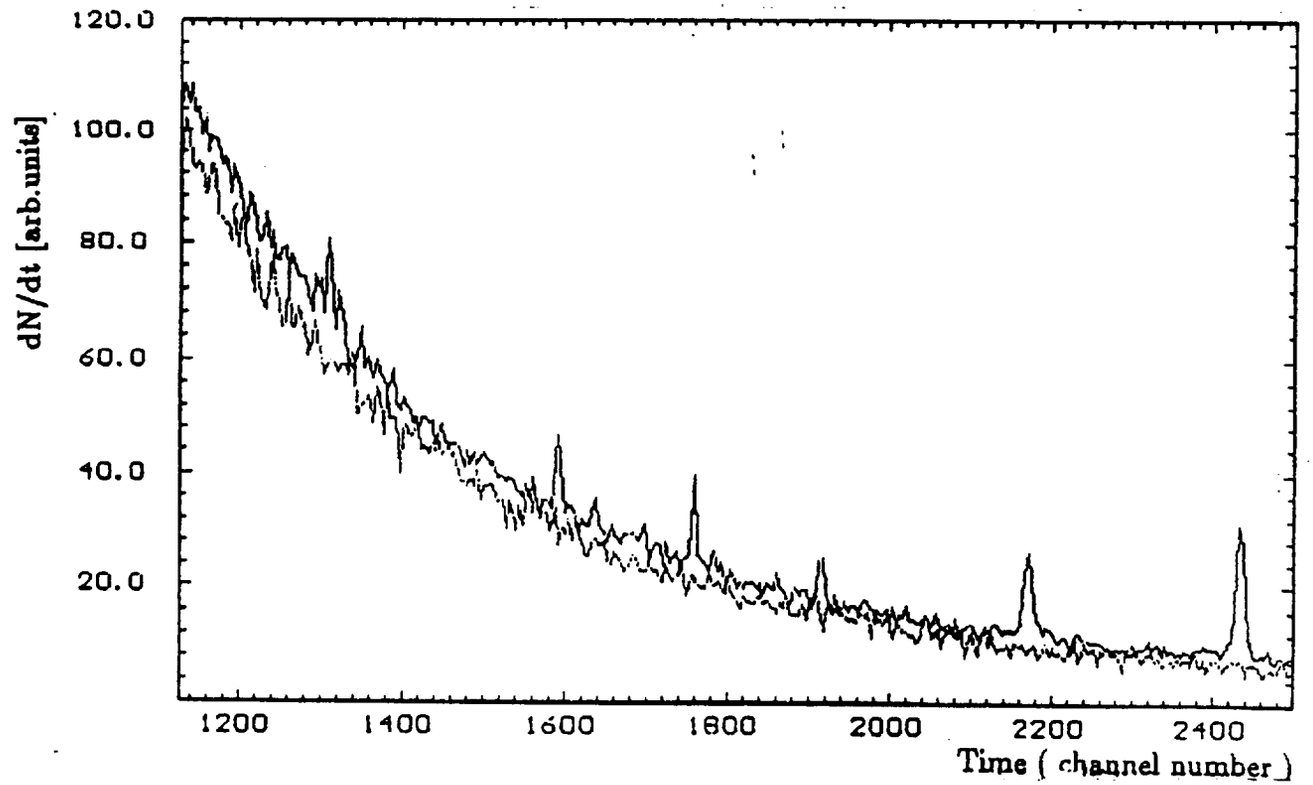

Fig.3 b. CSC TOF spectra with and without filter in the beam

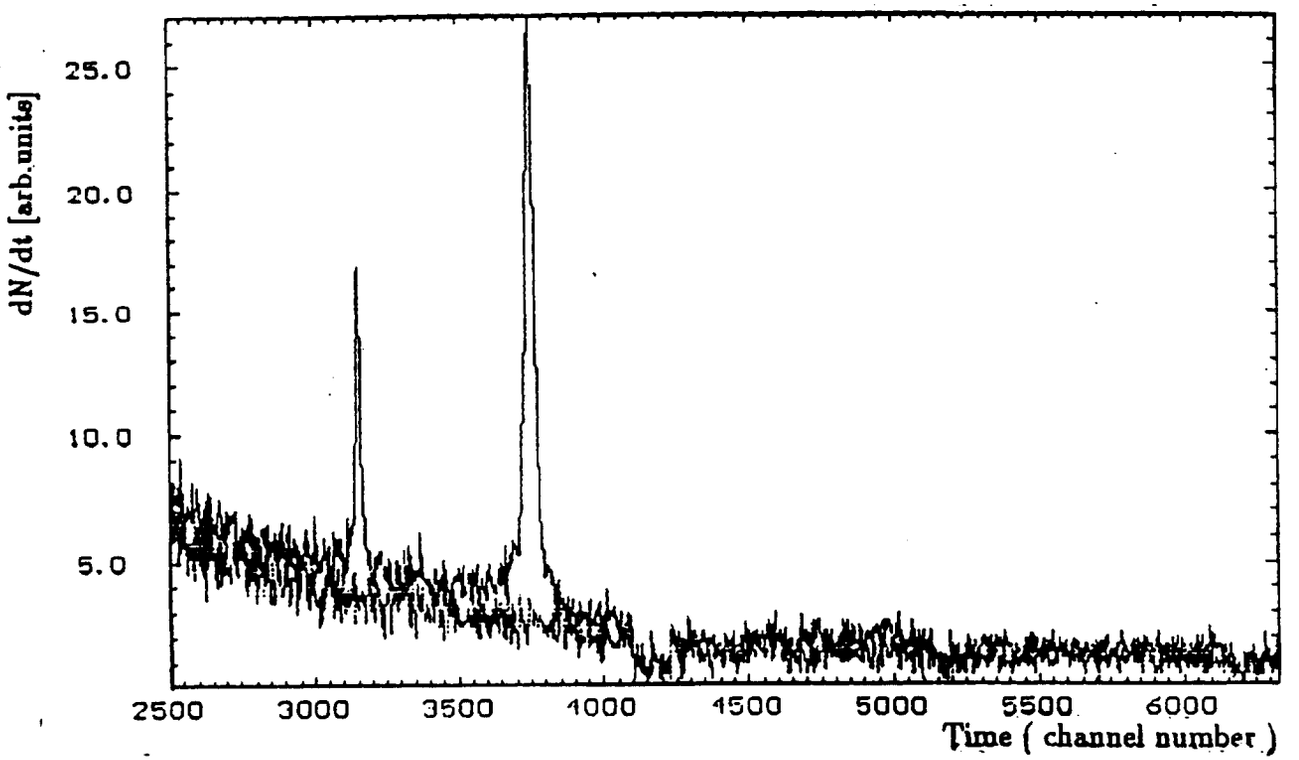

Fig.3 c. CSC TOF spectra with and without filter in the beam

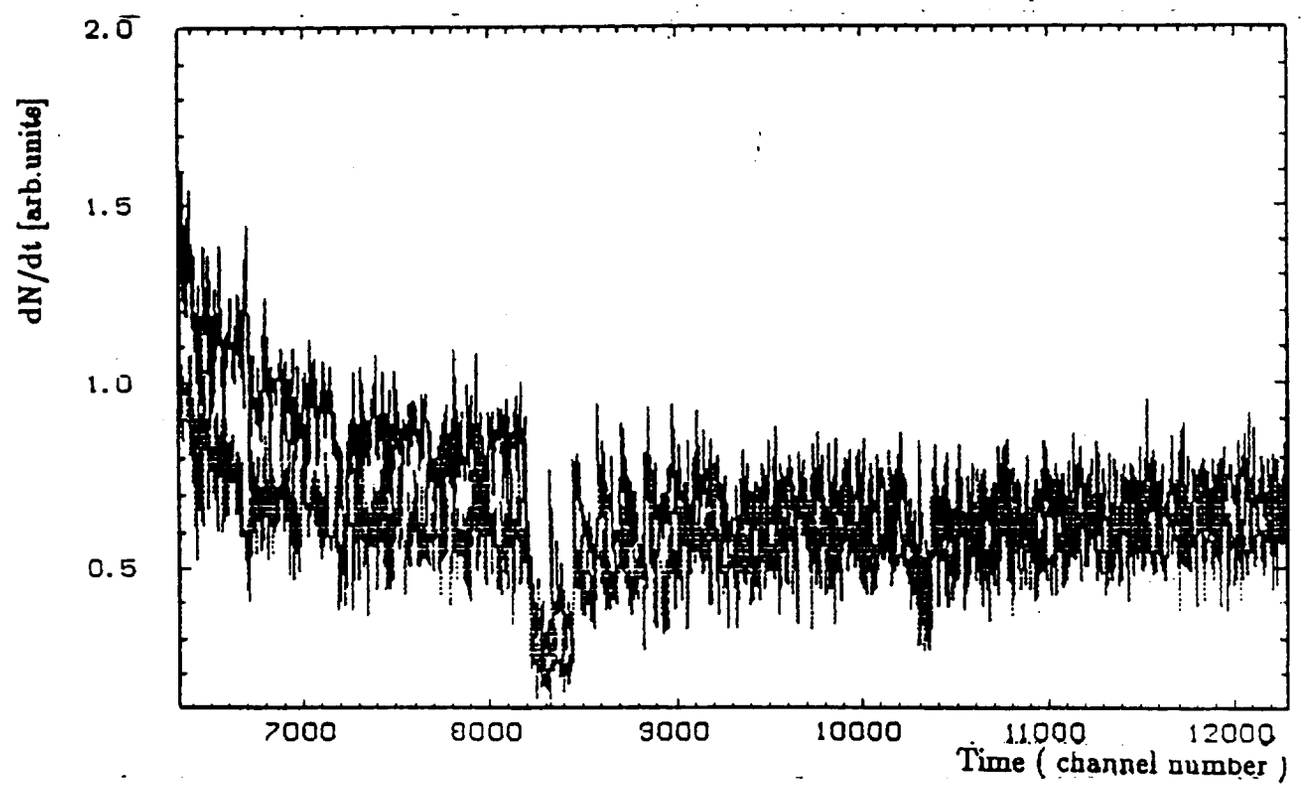

Fig.3 d. CSC TOF spectra with and without filter in the beam

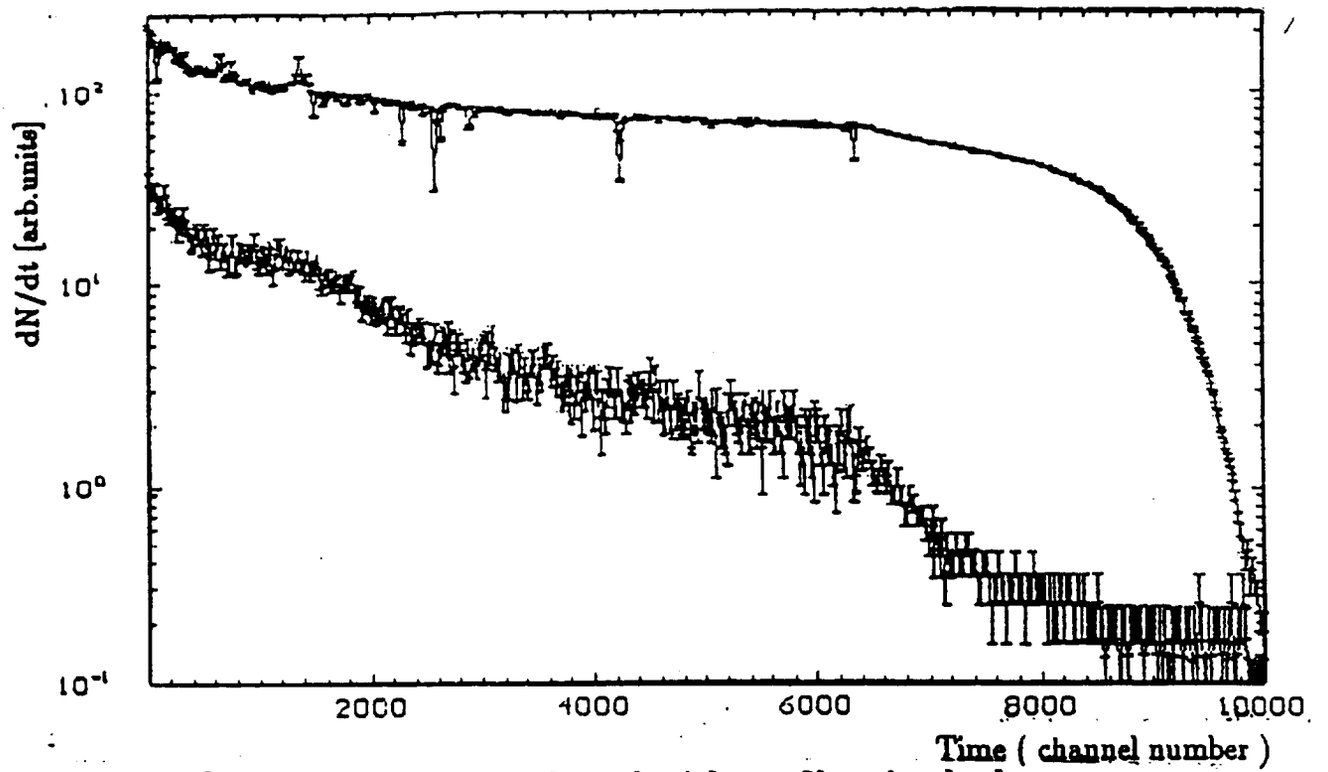

Fig.4 ^{3}He TOF spectra with and without filter in the beam

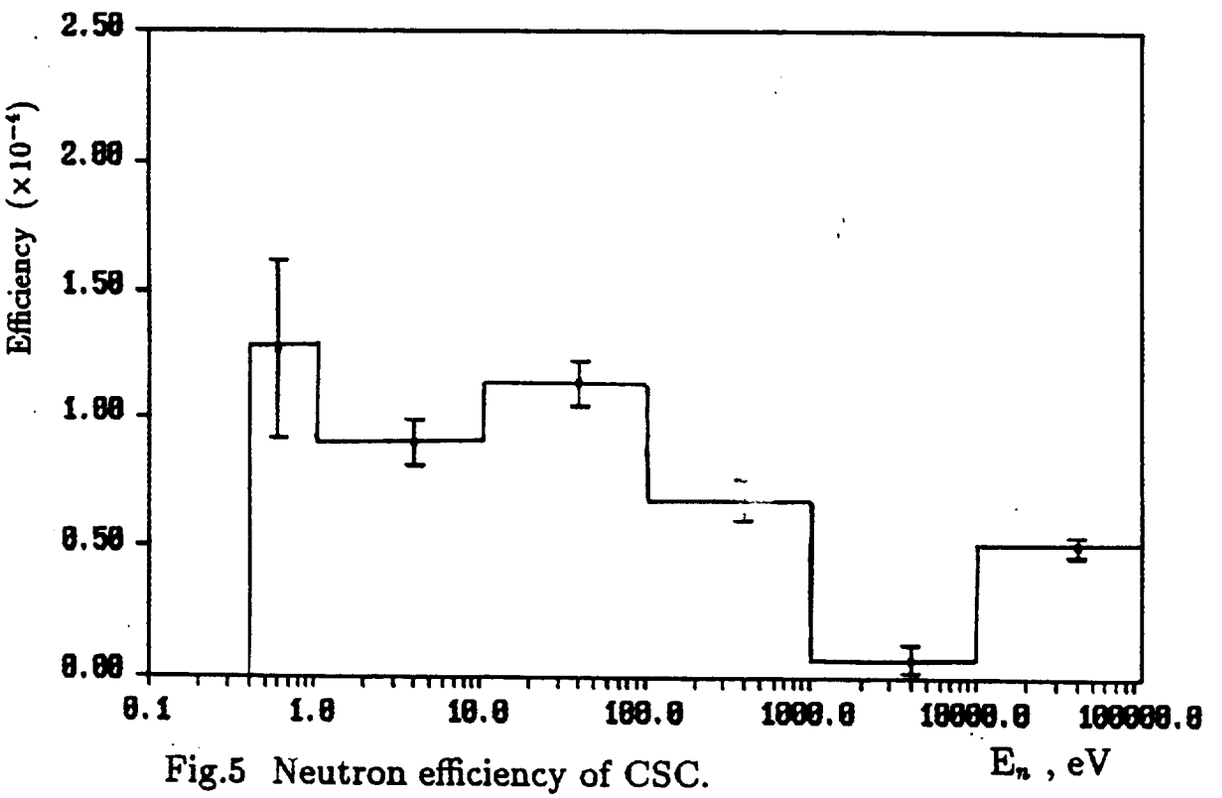

Fig.5 Neutron efficiency of CSC.

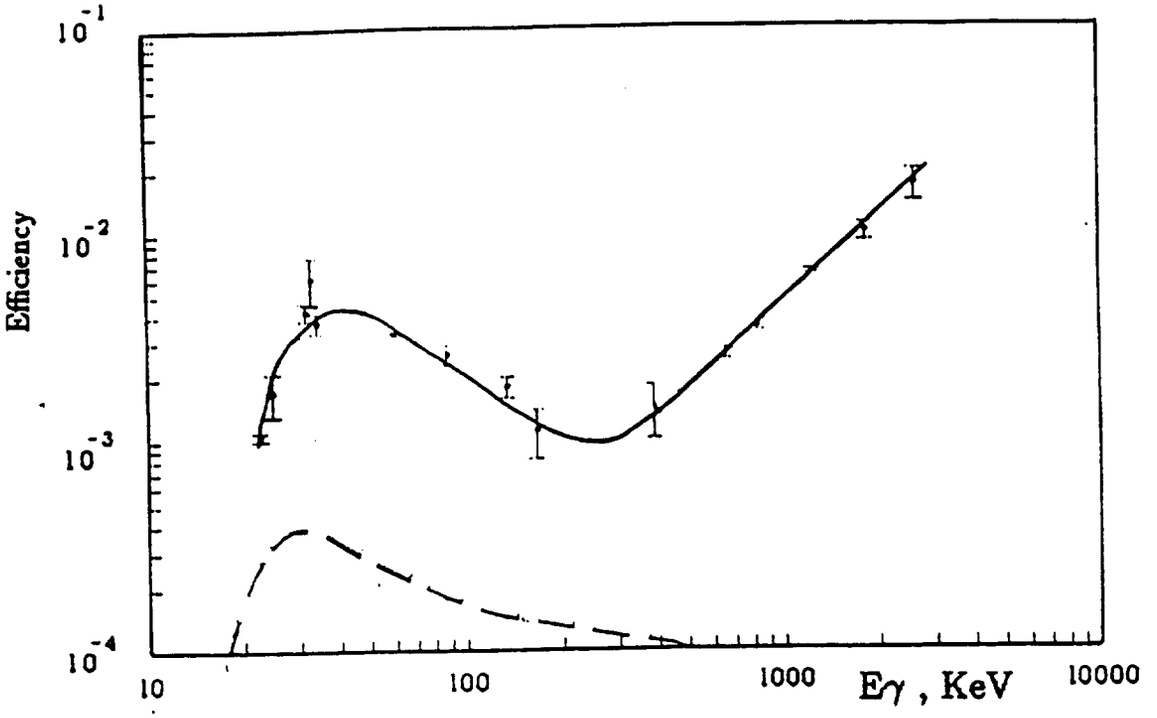

Fig.6 Gamma efficiency of CSC.The solid curve is the eye guide to the experimental data. The dashed curve is calclulated probability for the gamma absorbtion in the gas gap.

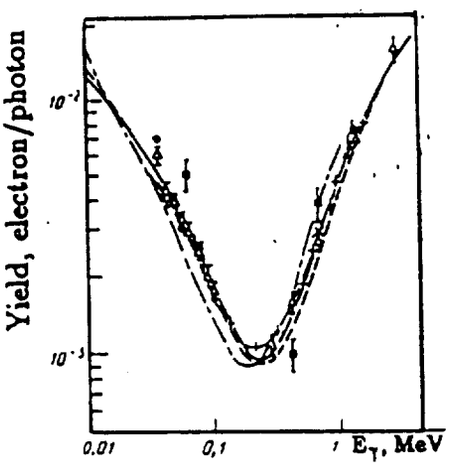

Fig.7 The yield of the secondary electrons ($E_\gamma > 50$ eV) from copper targets in function of the gamma energy. The curves are MC calculations. Note that the target thickness was varied to be equal to the range of the photoelectrons.